NRL Report 6779

Procedures for Fracture Toughness Characterization and Interpretations to Failure-Safe Design for Structural Titanium Alloys

R. J. Goode, R. W. Judy, Jr., and R. W. Huber

Strength of Metals Branch
Metallurgy Division

December 5, 1968

NAVAL RESEARCH LABORATORY
Washington, D.C.

This document has been approved for public release and sale; its distribution is unlimited.

CONTENTS

Abstract ii
Problem Status ii
Authorization ii

INTRODUCTION 1

METALLURGICAL CHARACTERISTICS OF TYPES OF TITANIUM ALLOYS 1

PHYSICAL METALLURGY ASPECTS 2

- Alpha Alloys 2
- Alpha-Beta Alloys 2
- Beta Alloys 3
- Oxygen in Titanium 3

FRACTURE TOUGHNESS TESTS 3

- Fracture Mechanics Tests 3
- C_v Test 6
- DT Test 6

CORRELATION OF FRACTURE TOUGHNESS TESTS 7

- Correlation of DT and C_v Tests 9
- Correlation of K_{Ic} and DT Tests 10
- Correlation of K_{Ic} and C_v Tests 12

GENERAL INTERPRETATION OF CORRELATION RELATIONSHIPS 12

- Fracture Toughness Diagram for Titanium Alloys 15
- Flaw Size Analysis Diagram 17
- Ratio Analysis Diagram 19

SUMMARY 22

ACKNOWLEDGMENTS 23

REFERENCES 23

APPENDIX — Characteristics of Commercially Produced Titanium Alloys Referenced in Report 24

ABSTRACT

Interpretations of fracture toughness characteristics, as measured by various test procedures, for solutions of general engineering problems are presented for structural titanium alloys. Analytical procedures evolved from fracture mechanics theory are used for quantitative interpretations of engineering fracture toughness tests. The procedural simplicity of the engineering tests coupled with the analytical capabilities of fracture mechanics theory provides for a significant advancement in failure-safe design procedures for titanium alloys covering the full range of strength levels.

Interpretative procedures are evolved from correlations of K_{Ic} with Dynamic Tear (DT) and Charpy-V notch (C_v) energy. An Optimum Materials Trend Line (OMTL) diagram is developed for titanium alloys which summarizes all the DT fracture toughness data and is additionally indexed according to the K_{Ic} and C_v correlation plots. The OMTL limit curves are shown for the best and normally expected grades of material for the strength level.

Flaw size-stress calculations for fracture of 1- and 3-in.-thick sections are overlayed to the OMTL diagram in the form of iso-flaw depth lines. K_{Ic}/σ_{ys} ratio lines are indexed to the iso-flaw depth lines, and a K_{Ic}/σ_{ys} Ratio Analysis Diagram (RAD) is evolved. The RAD provides for a simplified, general engineering interpretation of flaw size-stress conditions for fracture.

The general fracture toughness characteristics of some principal titanium alloys are simply defined by zones in the RAD. A compendium of such zones provides a general understanding of the potentials for each generic class of titanium alloys.

PROBLEM STATUS

This is a special interpretive report covering the results of a wide range of investigations within the Metallurgy Division of NRL, aimed at the general problem of metallurgical optimization and fracture-safe design. This is an interim report; work is continuing on the problem.

AUTHORIZATION

NRL Problems M01-05 and F01-17
Projects RR 007-01-46-5405, SF 51-541-004-12386,
SF 51-541-005-12393, and DSSP S-4607-1189

Manuscript submitted July 29, 1968.

PROCEDURES FOR FRACTURE TOUGHNESS CHARACTERIZATION AND INTERPRETATIONS TO FAILURE-SAFE DESIGN FOR STRUCTURAL TITANIUM ALLOYS

INTRODUCTION

Considerable interest exists in the use of thick-section titanium alloys for structural applications requiring materials of high strength-to-density ratios. An important factor in the failure-safe design of such structures is the fracture toughness characteristics of the material. Until recently fracture toughness information for intermediate- and high-strength titanium alloys was available only for material of sheet thickness.

This report presents a summary of the fracture toughness characteristics of titanium alloys produced as plate of relatively large dimensions. It also presents procedures for the interpretation of fracture toughness tests in terms of critical flaw size and stress level factors for sections of 1- to 3-in. thickness. The procedures are based on correlations of Charpy-V notch (C_v) and Dynamic Tear (DT) tests with fracture mechanics tests in the range where valid intensity values of plane strain stress (K_{Ic}) can be established. Extrapolations of the correlations are used to cover conditions of higher fracture toughness. The correlation and interpretative procedures are the same as have been described previously for steels (1). Flaw size-stress calculations based on the fracture mechanics parameters K_{Ic} and K_c provide for the desired quantitative interpretations of the C_v and DT tests. The procedural simplicity of the engineering tests is thereby coupled with the analytical capabilities of fracture mechanics theory.

METALLURGICAL CHARACTERISTICS OF TYPES OF TITANIUM ALLOYS

Commercial titanium alloys are of three basic types: alpha, alpha-beta, and beta. The alpha (α) phase has a hexagonal-close-packed crystal structure and is the low-temperature allotropic transformation phase. The beta (β) phase is the high-temperature phase and has a body-centered-cubic crystal structure.

The α peritectoid system is typical for titanium alloyed with the α stabilizers aluminum, oxygen, nitrogen, and carbon. These elements have a high solubility in α, causing an increase in a solute content which raises the β transus temperature. The elements are all solid solution strengtheners in the α phase. Aluminum enters the titanium atomic lattice as a substitutional element, replacing titanium atoms. Oxygen, nitrogen, and carbon form interstitial solid solutions with titanium and occupy the vacant spaces existing between the titanium atoms in the crystal structure. Aluminum is a basic alloying element for practically all titanium alloys, since it decreases the density of the alloy and at the same time substantially strengthens the α phase without degrading weldability and fracture toughness.

Beta stabilizing elements have a high solubility in β titanium, have limited solubility in α titanium, and lower the β transus temperature with increasing alloy content. The elements iron, manganese, silicon, chromium, copper, and hydrogen are all strengtheners of the β eutectoid type. The elements molybdenum, vanadium, columbium, and tantalum are strengtheners which form the β isomorphous-type system and have unlimited solubility in the β phase.

The neutral alloying elements tin and zirconium have high solubility in both α and β titanium. They are relatively moderate solid solution strengtheners which do not appreciably change the β transus temperature.

PHYSICAL METALLURGY ASPECTS

Alpha Alloys

Alpha alloys are essentially all α phase at room temperature, even when rapidly quenched from temperatures well above the β transus. Usually small amounts of the β phase can be found due to impurities, such as iron, manganese, and silicon. If the combined amount of these elements is above 0.3%, the amount of β phase formed may affect the metallurgical character of these alloys. Heat treatment of these alloys can have considerable effect on fracture toughness, but the response with respect to strength is relatively small. The useful yield strength range of thick-section α alloys (0.08 maximum oxygen) is below 120 ksi. In general, α alloys are considered to have good welding characteristics. Typical α alloys are titanium containing fixed amounts of oxygen for increased strength, usually referred to as "commercially pure" titanium and Ti-5Al-2.5Sn.

Alpha-Beta Alloys

Alloys of the α-β type can be subdivided into two groups. Alloys containing β stabilizing elements in amounts sufficient to impart only a limited amount of heat-treatment response with respect to strength are termed near-α (or super-α) alloys, since their metallurgical character closely resembles that of α alloys. The factors discussed for α alloys apply equally well to near-α alloys. Ti-6Al-2Cb-1Ta-0.8Mo is a typical near-α alloy.

Alloys containing β stabilizing elements sufficient in amount to impart a high degree of heat-treatment response are termed α-β alloys. Those alloys containing less than about 5% β stabilizing elements range from about 115-ksi yield strength in the annealed condition to about 150-ksi yield strength in the heat-treatment condition. Alpha-beta alloys containing greater amounts of β stabilizing elements are heat treatable to close to 200-ksi yield strength from an annealed yield strength of approximately 125 to 130 ksi. Intermediate strengths are obtained by varying the heat-treatment conditions. In general, an increase in the amount of β stabilizing elements in α-β alloys (i.e., increase in β phase present) results in a decrease in fracture toughness.

Strengthening of α-β alloys is accomplished by solution annealing high in the α-β region or in some cases above the β transus temperature, followed by a rapid cool to room temperature. The solution-annealing temperature determines the amount and composition of the β phase which is retained in an unstable condition at room temperature. Aging treatments in the range of 900 to 1200°F precipitates α titanium from the β phase, which enriches the β phase in β stabilizing elements and results in increasing its stability.

The weldability of α-β alloys decreases with increasing amounts of β stabilizing elements. For example, welds in the alloys Ti-6Al-4V and Ti-6Al-2Mo (or Ti-7Al-2.5Mo) can be made to match the plate properties, if proper protection against oxygen contamination is applied, whereas weldments with inferior ductility and fracture toughness properties compared to plate are generally obtained for an alloy such as Ti-6Al-6V-2.5Sn-1Cu-0.5Fe (normally designated Ti-6Al-6V-2.5Sn).

Beta Alloys

Alloys containing sufficient alloying elements to cause only β titanium to exist in the alloy at ambient temperature are called β alloys. These alloys are metastable and are classified as eutectoid or compound-free alloys. When moderately heated for extended times, the β phase of the eutectoid-type alloys will sluggishly transform and precipitate a compound due to eutectoid decomposition. The α phase is precipitated from the β phase of the compound-free-type alloys. In general, β alloys can be heat treated into the same strength range as α-β alloys.

Few β alloys have been produced on a commercial basis. In general, they have been designed for ultrahigh strength and display relatively poor fracture toughness properties at moderate strengths. The low toughness is due primarily to the high content of β stabilizing elements in these alloys.

The only current commercial β alloy is the eutectoid-type Ti-13V-11Cr-3Al. This alloy is considered weldable. As welded, the welds are fairly ductile with a fracture toughness equivalent to annealed plate. However, it has the problem of low ductility and low fracture toughness in the weld compared to the plate when heat treated to high strength levels.

Recent developments for the compound-free β alloys Ti-11Mo-5.5Sn and Ti-11Mo-5Sn-5Zr indicate that significant improvements in fracture toughness and weldability may be expected in β alloys in the near future.

Oxygen in Titanium

All commercial titanium alloys contain oxygen in substantial amounts. Some of the oxygen is contained in the titanium sponge used for melting into ingots. It is not eliminated or reduced in the vacuum melting process. Furthermore, oxygen is often added to increase the strength of the material. Thus, for all practical purposes, oxygen is an alloying element in titanium and is considered as such in this report.

In line with its role as a potent strengthener, oxygen seriously affects the fracture toughness of titanium alloys — especially in thick sections. As a general approximation, it is desirable to keep the level of oxygen below 0.08% for optimization of fracture toughness. Fracture toughness deteriorates rapidly with increasing oxygen above 0.08%; the critical level of oxygen appears to vary slightly for different alloys. To date, all available data indicate that the commercially designated extra low interstitial (ELI) grade alloys, which contain from 0.10% to 0.13% oxygen and especially the alloys of standard commercial purity (0.15% to over 0.2% average oxygen content), fall well below the maximum level of fracture toughness observed for the very low oxygen alloys.

The data in this report relate to rolled plate produced from commercial double-vacuum-arc melted ingots. The level of oxygen was maintained below 0.08% except for a few cases where limited amounts of ELI and standard commercial purity material were investigated. The chemical composition and range of yield strength investigated are listed in the Appendix for the different alloys.

FRACTURE TOUGHNESS TESTS

Fracture Mechanics Tests

Fracture mechanics tests characterize fracture toughness in terms of the value of the elastic stress field intensity K in the region ahead of the crack-tip plastic zone at

the point of instability. The critical stress intensity level for crack extension is designated by the parameter K_{Ic}. The subscript I defines conditions of the "opening" mode (2) for which the applied stress is normal to the crack.

Values of K are calculated from experimental determinations of crack-tip opening displacements obtained by means of a clip gage spanning the crack opening. Load-vs-clip-gage displacement plots provide the indication of a crack-tip-opening instability by a drop in the load with increasing clip gage displacement. The nominal stress is calculated using appropriate beam equations. The critical stress intensity factor for instability K_{Ic} is then derived from fracture mechanics equations which relate K to crack depth and nominal stress. Crack instability occurs at a value of K_{Ic} which is unique to the material. Different combinations of crack depth and nominal stress can be used to obtain this value, provided plane strain conditions are satisfied.

The K_{Ic} value must be measured under the condition of plane strain, i.e., the maximum possible mechanical constraint that can be applied to the metal at the crack tip. When this condition is attained, K_{Ic} represents the lowest value of fracture toughness and is said to be "geometry independent." In K_{Ic} testing, plane strain is attained by imposing predetermined requirements on the width, length, thickness, and crack depth of the fracture mechanics specimens to ensure valid plane strain values are obtained. Of these requirements, thickness is most significant to valid K_{Ic} determinations in that it is the basic dimension from which other conditions required for maximum mechanical constraint are determined. For example, increased thickness is required with an increase in fracture toughness to provide for flaw dimensions (width and depth) sufficient to maximize constraint conditions at the crack tip. Once a valid plane strain K_{Ic} fracture toughness value has been determined, it is then possible to calculate critical flaw size-stress level relationships for various kinds of flaws based on equations derived by linear elastic fracture mechanics. The calculations presuppose that equivalent conditions of maximum constraint are involved. The thickness of the K_{Ic} specimen must meet the conditions of the following expression to ensure plane strain:

$$B \geq 2.5\ (K_{Ic}/\sigma_{ys})^2 ,$$

where B is the thickness (in.), K_{Ic} is the critical plane strain stress intensity factor (ksi $\sqrt{\text{in.}}$) and σ_{ys} is the yield stress (ksi).

It is important to note that the ratio of $(K_{Ic}/\sigma_{ys})^2$ is proportional to the crack-tip plastic zone size. According to this ratio, for a constant K_{Ic} value, increased yield strength results in a decrease in the plastic zone size, i.e., decrease in fracture toughness. An increase in K_{Ic} for a given level of yield strength rapidly increases the plastic zone size and, therefore, the B requirement for retention of the plane strain condition. Thus, for materials of high fracture toughness the required specimen size becomes very large, because the $(K_{Ic}/\sigma_{ys})^2$ ratio is increased. For example, a material with a ratio of 2.0 in. requires a B value of at least 10 in.

If the thickness is less than the minimum B requirement, the mechanical constraint is then less than adequate for plane strain (even for a very deep crack), and the measurement of fracture toughness must be considered as relating to a specimen-geometry-dependent K_c value. Mathematical relationships between K_c and K_{Ic} parameters have been proposed for calculation of the K_{Ic} stress intensity factor measured under K_c conditions and vice versa. However, these relationships are considered only as approximations at the present stage of development of fracture mechanics. For metals of relatively high fracture toughness (high ratios of K_{Ic}/σ_{ys}) the relationships provide for calculations of plane stress critical flaw sizes which are very large and, therefore, do not place a premium on exactness. Such calculations may be regarded as estimates which provide helpful guidelines for general engineering use of relatively tough materials.

At the present stage of development, fracture mechanics tests do not lend themselves to routine testing. The cost of K_{Ic} testing is high due to the requirement of close tolerances on specimen dimensions, stringent conditions for producing acceptable fatigue cracks, and other aspects of research laboratory equipment and procedures required in the conduct of the tests.

Because of the limitations of fracture mechanics testing, considerable benefit would be derived from a correlation of K_{Ic} values with the results of simple engineering tests which can be used for routine fracture toughness characterization. The engineering tests may be used across a full spectrum of fracture toughness conditions ranging from plane strain to full plane stress. Within the limits of geometry factors which provide for valid K_{Ic} measurement, direct correlations between the tests should be possible. Beyond the limits for which valid K_{Ic} values can be obtained, extrapolation of the correlations can be made to provide approximations of the K_{Ic} value. In effect, this procedure is equivalent to that used for obtaining "corrected" K_{Ic} values by calculation based on plastic zone size corrections. For intermediate to high fracture toughness, the correlated or approximated K_{Ic} value is then used for calculating critical flaw size-stress levels for instability with the added consideration of the effects of plane stress. Essentially, this procedure involves a reverse adjustment by calculations based on K_{Ic}-K_c relationships to represent the effective K_c condition expected for the thickness and flaw sizes in question.

The problem of conducting valid K_{Ic} tests and the interpretations for tests relating to tough materials is a complex subject which is covered in a simplified introductory manner in Ref. 1.

A variety of fracture mechanics tests are available for obtaining valid K_{Ic} data (3), provided the requirements for plane strain are met. For the investigations to be described, the single-edge-notch (SEN) tensile specimen dimensioned for testing of 1-in.-thick plate was used. The specimen was grooved on each side along the expected fracture path to a depth of 5% of the thickness to provide enhanced detectability of the point on the load-vs-displacement curve at which crack instability occurred. A 0.10-in.-deep fatigue crack was formed at the bottom of a 1.5-in.-deep machined notch in accordance with best practices. The clip-type displacement gage was inserted into machined grooves at the surface of the notch to measure the crack-opening displacements. The SEN specimen is illustrated in Fig. 1.

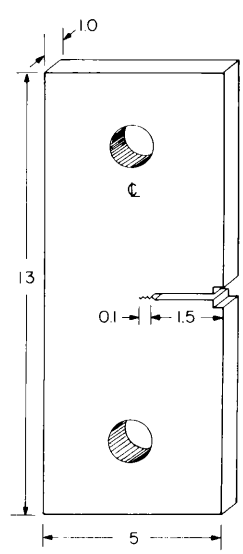

Fig. 1 - Single-edge-notch (SEN) fracture mechanics tensile specimen used for K_{Ic} studies (dimensions proportional to thickness)

Load-vs-displacement curves were obtained with an X-Y recorder from the outputs of a load sensor on the tensile machine and the crack-opening displacement gage. When initial deviation from linearity (crack instability) occurred at or very near maximum load, this value was used to calculate K_{Ic}; otherwise, the load at the lowest distinct deviation from linearity was used. A one iteration correction for plastic zone size was included in the K_{Ic} calculations.

C_v Test

The C_v test is the standard fracture toughness test used by the steel and titanium industry. Unfortunately, the C_v test has been found to have serious limitations of interpretation for both steels and titanium alloys. The test must be indexed by other large-scale tests or by correlation with service experience for various types of steel in the temperature range corresponding to the transition from low to high fracture toughness. For titanium alloys, the C_v test is less discriminating than other fracture toughness tests — especially in the region of low fracture toughness.

DT Test

The DT test was developed to provide a practical laboratory procedure for measurement of the fracture toughness associated with the characteristic fracture propagation mode of the metal. A principal requirement for this purpose, which is a feature of the DT test, is the simulation of a sharp natural crack for the initiation of the fracture. This feature is obtained for the DT test by the simple expedient of introducing a brittle electron beam (EB) weld, thereby eliminating the complications of fatigue precracking. The energy required to fracture the specimen serves as an index of the size of the crack-tip plastic zone associated with the natural process of fracture propagation. For relatively brittle materials which fracture in the plane strain mode (flat fracture) a small plastic zone is indicated, and low energy absorption is measured. With increasing toughness, the plastic zone size increases, culminating in the development of a large plastic enclave preceding the fracture process; therefore, higher fracture energies are obtained with corresponding increase in the amounts of slant fracture (shear).

Mechanical constraint effects due to thickness which influence the plastic zone size may be evaluated directly by scaling the size of the DT specimen. The width-to-thickness geometry of the DT test is liberally sufficient to establish conditions for the development of the natural fracture mode related to intrinsic toughness and thickness aspects. In effect, the test defines the fracture mode (plane strain, mixed-mode plane stress, or full plane stress) when conducted for the specific section size of interest.

The interpretation of the effects of deviations from the specific size depend on the intrinsic fracture toughness that is observed. For example, a flat break (square) fracture which implies plane strain conditions would not be changed by increased thickness. Similarly, a full-slant plane stress fracture, associated with high energy absorption measured for a 1-in. DT test, implies that an increase to sections of 2- to 3-in. thickness would not decrease the fracture toughness level (due to mechanical constraint) sufficiently to change the characterization of the thick-section fracture toughness as related to gross strain mechanical conditions. For intermediate fracture toughness levels represented by mixed-mode plane stress fractures, the effects of changes in section size require more detailed assessment for purposes of engineering interpretation. Studies of section-size effects are being conducted to corroborate other deductions that may be made from fracture mechanics calculations.

Because the natural event of fracture which is measured by any fracture toughness test is energy, it should be expected that measurements of the energy to fracture in the

DT test should be indexable accurately to fracture mechanics K_{Ic} tests for conditions involving plane strain or for reasonable deviations from plane strain. For mixed-mode K_c fracture conditions in which K_{Ic} correction calculations must be made for fracture mechanics tests because of inadequate thickness constraint, increased DT energy is obtained which corresponds to the K_c increase. For conditions of full slant fracture, the much higher DT energy relates to full plane stress K_c conditions. This condition of high fracture toughness can be represented as an approximation of the K_{Ic} value derived by extrapolation of the correlation data. Subsequent K_c calculations derived from the approximated K_{Ic} value serve to indicate conditions related to very large flaw sizes and plastic loads. The estimates appear to be reasonable as indicated by separate correlations of DT test fracture resistance to Explosion Tear Test (ETT) performance. In effect, the full plane stress K_c conditions translate to flaw size and stress calculations of such a magnitude so as to be of no concern except for conditions of gross plastic overload and huge flaw sizes.

A schematic of the DT specimen for 1-in.-thick titanium plate is shown in Fig. 2. An EB weld, embrittled by diffusing in iron during the welding operation to form a Ti-5%Fe alloy, is used to generate the desired deep, sharp crack. Impact loading with a calibrated falling or swinging weight is used to fracture the specimen and measure the energy absorbed. The DT test value is ordinarily taken as the energy required to fracture a specified area of plate material.

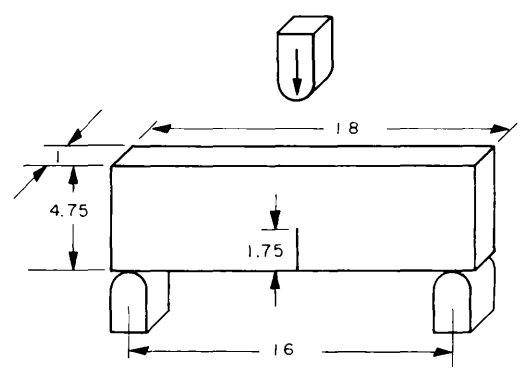

Fig. 2 - DT test specimen for 1-in.-thick plate material. An EB weld, embrittled by diffusing in iron during the welding operation to form a Ti-5TFe alloy, is used to generate the desired deep, sharp crack (dimensions in inches).

The brittle crack-starter weld of the DT specimen also serves to provide a limit-severity test condition for strain-rate-sensitive materials. Strain-rate sensitivity effects are thus integrated into the DT energy value measured. If the material is not strain rate sensitive, the brittle weld is equivalent to a deep fatigue crack in the specimen.

The general fracture surface appearance of DT specimens for extremes in fracture toughness for titanium alloys is shown in Fig. 3. The flat fracture (Fig. 3a) corresponds to brittle (plane strain) behavior and low DT values. Very high levels of toughness correspond to conditions of plane stress for which high DT values and slant fracture (Fig. 3b) are obtained.

CORRELATION OF FRACTURE TOUGHNESS TESTS

Correlations have been developed between the K_{Ic} and DT fracture toughness tests using 1-in.-thick specimens. Correlation possibilities between the standard C_v specimen and the K_{Ic} and DT tests have also been investigated.

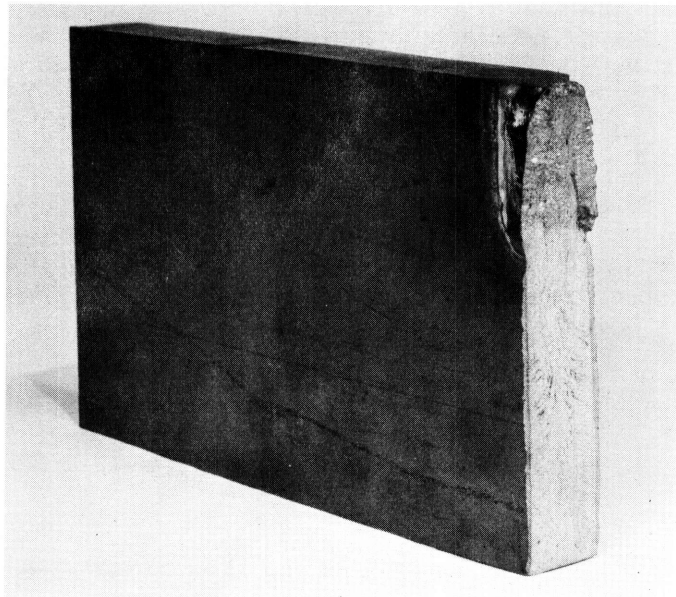

(a)

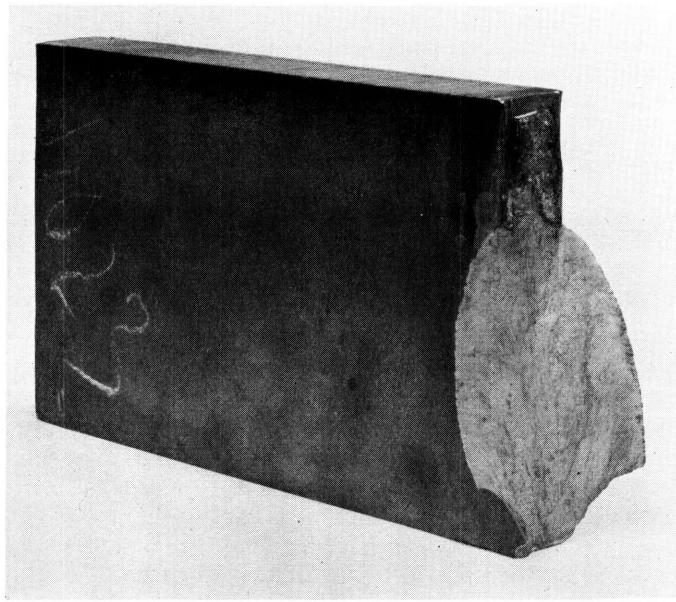

(b)

Fig. 3 - DT fracture appearance for (a) low fracture toughness and (b) high fracture toughness titanium alloys in 1-in.-thick plate

The K_{Ic} tests were conducted for selected α-β alloys, which when heat treated could be expected to cover a wide range in yield strength and K_{Ic} values. Insofar as possible, alloys with optimum combinations of strength and toughness as defined in the DT test were used to provide information on the upper limit of K_{Ic} values than can be expected for different levels of yield strength with current alloys. A much larger number of the alloys have been investigated in the C_v and DT tests for correlation between these two tests.

In previous studies, the significance of the DT and C_v values was established (4) by extensive indexing with the ETT, which served as a structural prototype test. This test features a 2-in.-long through-thickness brittle EB crack-starter weld, similar to the DT test brittle weld, centrally located in a 1-by-22-by-25-in. plate. Upon explosive loading, the plate bulges to conform to a cylindrical shape. The amount of plastic deformation which develops serves as an index of the level of crack propagation resistance of the material in the presence of a large flaw. The typical performance of high, intermediate, and low fracture toughness material in the ETT is illustrated in Fig. 4. The fracture modes relate to full plane stress, mixed-mode plane stress, and plane strain, respectively. These fracture modes were reproduced exactly by the DT tests.

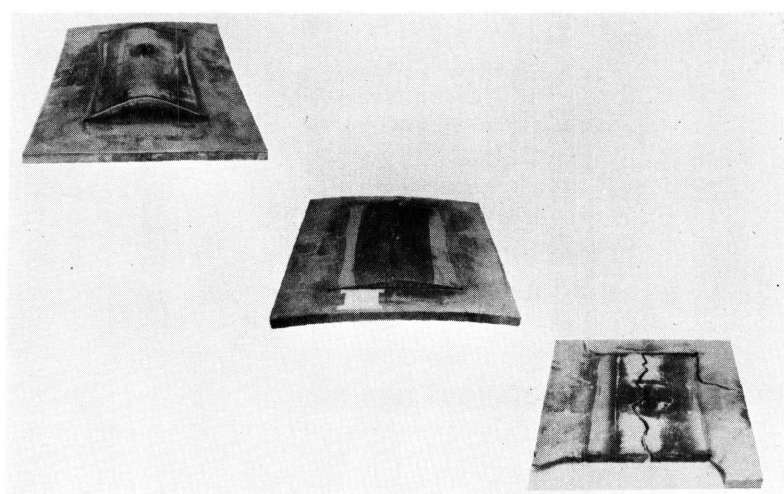

Fig. 4 - ETT of plates 1 by 22 by 25 in. featuring a 2-in.-long through-thickness brittle crack-starter weld. The series indicates the dramatic decrease from high to intermediate to low fracture toughness

The DT-vs-ETT correlations for high levels of fracture toughness serve to validate the approximations used to correlate DT energy to apparent K_{Ic} values as determined from plate thickness of less than adequate B for valid determination of K_{Ic} values. The calculations to K_c conditions which are made for the high fracture toughness range from the apparent K_{Ic} values are in line with the performance observed in ETT tests.

Correlation of DT and C_v Tests

The relationship between DT and C_v fracture energies is shown in Fig. 5. The correlation band shows a general trend of increasing C_v values with increasing DT energy. It is apparent that only rough interpretations of the C_v values can be made with

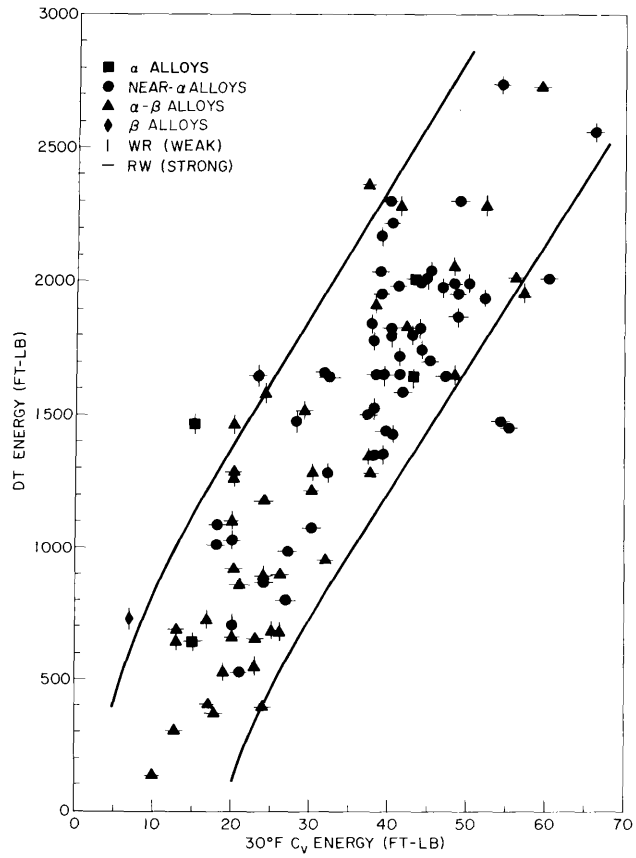

Fig. 5 - Correlation of DT and C_v energy values for 1-in.-thick plate

respect to the full spectrum of fracture toughness. The C_v values below 20 ft-lb generally correspond to DT energy values below 1000 ft-lb. Values of 25 to 45 ft-lb C_v energy would normally be expected in the DT energy range of 1000 to 2000 ft-lb. Values of 50 to 70 ft-lb C_v energy would be expected for DT values between 2000 to 3000 ft-lb.

Correlation of K_{Ic} and DT Tests

A plot of K_{Ic} as a function of yield strength is shown in Fig. 6. The chart indicates that an inverse relationship exists between K_{Ic} fracture toughness and yield strength. This relationship corresponds to more extensive data available for high-strength sheet material. A poorly defined K_{Ic}-Optimum Materials Trend Line (OMTL) curve evolves because of selection of the best material which defined the DT-OMTL curve (shown later in Fig. 12). In effect, both tests define a dramatic decrease in the limit level of fracture toughness with increased yield strength.

In Fig. 7, K_{Ic} is plotted as a function of DT energy. It is apparent that an increase in K_{Ic} values is associated with a corresponding increase in DT energy values. Values of K_{Ic} in excess of 140 ksi $\sqrt{\text{in.}}$ could not be measured for specimens of 1-in. thickness. For the yield strength levels involved, the required B values are greatly in excess of 1 in. This follows because the $B > 2.5(K_{Ic}/\sigma_{ys})^2$ requirement would exceed values of 1 in. This indicates that the natural controlling fracture toughness for a 1-in. plate of this high level of intrinsic fracture toughness is a K_c plane stress condition. If plate material of 2- to

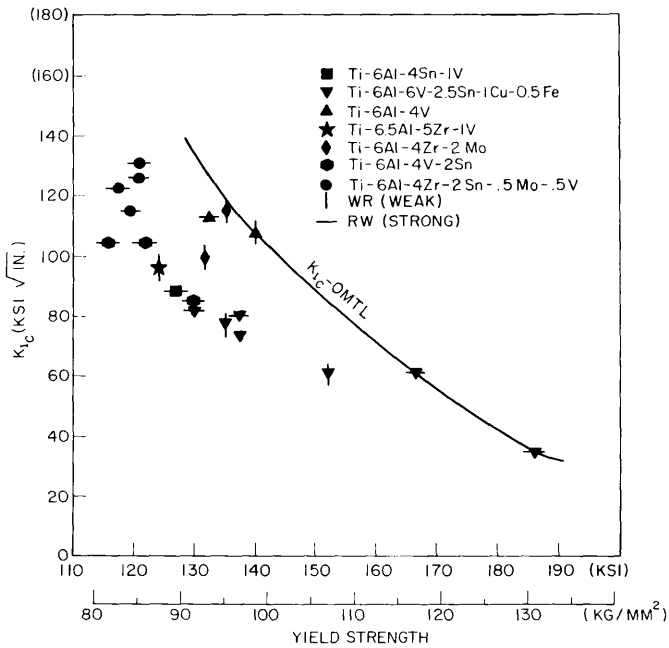

Fig. 6 - Relationship of K_{I_c} values to yield strength for 1-in.-thick plate

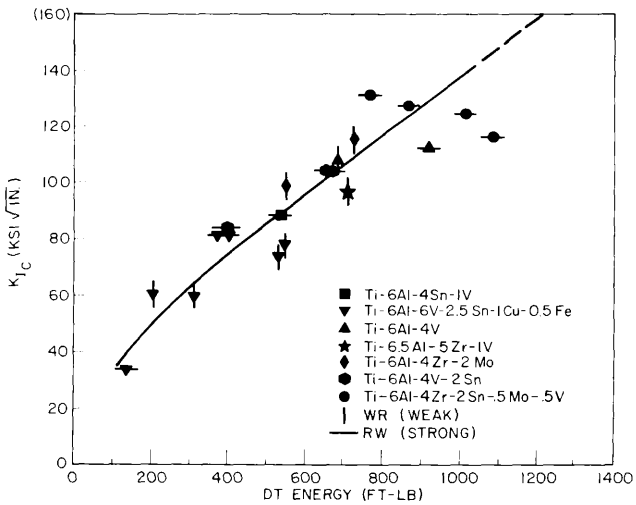

Fig. 7 - Correlation of K_{I_c} and DT test values for 1-in.-thick plate

3-in. thickness retained this level of metallurgical fracture toughness, a possibility exists that K_{Ic} values corrected for plastic zone size could be obtained. The curve in Fig. 7 is extrapolated above the 140-ksi $\sqrt{in.}$ value to provide estimates of the K_{Ic} correlation for thicker material. As data become available for thick-section alloys, corrections to these relationships will be applied as required.

The slope of the K_{Ic}-vs-DT energy plot appears to be steeper for the brittle materials than for the tougher materials. This change in slope indicates that for tougher materials the DT energy is increasing more than the K_{Ic} value due to an increasing influence of plane stress on the DT fracture propagation process.

The determination of K_{Ic} is made primarily from initial crack instability which for a tough material is measured under conditions in which the restraint effects of the crack remain partially operative. After the initial instability, relaxation of the crack-tip constraint is a natural event for both the K_{Ic} and DT tests. In effect the DT test provides a more reliable index of increasing fracture toughness as related to propagation of the fracture. The K_{Ic} value is more related to conditions of initial instability which may not apply after the "first event" measurement is made. This has the effect of decreasing the slope of the correlation curve as materials of higher fracture toughness come into consideration.

The strain energy release rate $\mathcal{G}_{Ic}$ is related to DT energy as shown in Fig. 8. In this plot, the DT energy is divided by the nominal fracture area (excluding the brittle weld) to compare the same quantity on each axis. This comparison corroborates that both tests are providing a reasonably equivalent measure of plastic zone sizes for conditions involving the determination of reasonably reliable K_{Ic} values. The plastic zone size is the basic parameter which relates to DT energy and to the K_{Ic} value or, more correctly, to $(K_{Ic}/\sigma_{ys})^2$.

Correlation of K_{Ic} and C_v Tests

The correlation of K_{Ic} with C_v energy is shown in Fig. 9. Although the chart shows a scatter of C_v data for high K_{Ic} values and very limited data for low-value materials, a general trend of increasing C_v energy with increasing K_{Ic} is indicated. The scatter in the correlation was not reduced to the same degree that had been observed previously for steels when normalized on the basis of yield strength. This is another indication that the fracture toughness discrimination potential of C_v tests for titanium alloys is poor compared to that of the DT test.

GENERAL INTERPRETATION OF CORRELATION RELATIONSHIPS

The aim of these investigations was the use of fracture mechanics analytical procedures for characterizing the fracture toughness of titanium alloys in terms of critical flaw size-stress level features required for fracture. The correlations of the C_v and DT tests to K parameters provide the basis for this two-step approach. While the relationships are approximate for conditions of intermediate and high fracture toughness, the size of the flaws and stress levels involved rapidly attain proportions such that high accuracy is not required.

The two-step analytical procedure was evolved recently and documented in detail for steels (1). As a first step, a master OMTL diagram based on DT data was indexed by the correlations to the C_v and K_{Ic} scales. The DT data defined an OMTL limit curve which indicated the highest level of toughness which had been attained for steels for any given level of yield strength. A normal expectancy OMTL was also deduced which indicated the level of fracture toughness that could be obtained with a high degree of confidence when

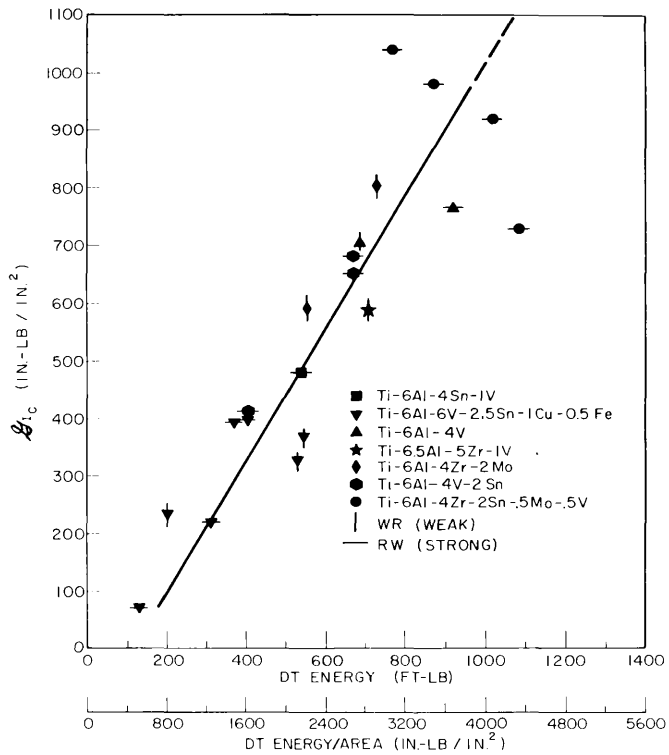

Fig. 8 - Correlation of $\mathcal{G}_{Ic}$ and DT fracture energy per unit area for 1-in-thick plate. $\mathcal{G}_{Ic}$ is a measure of energy released due to fracture and is mathematically related to K_{Ic} and to the K_{Ic}/σ_{ys} ratio.

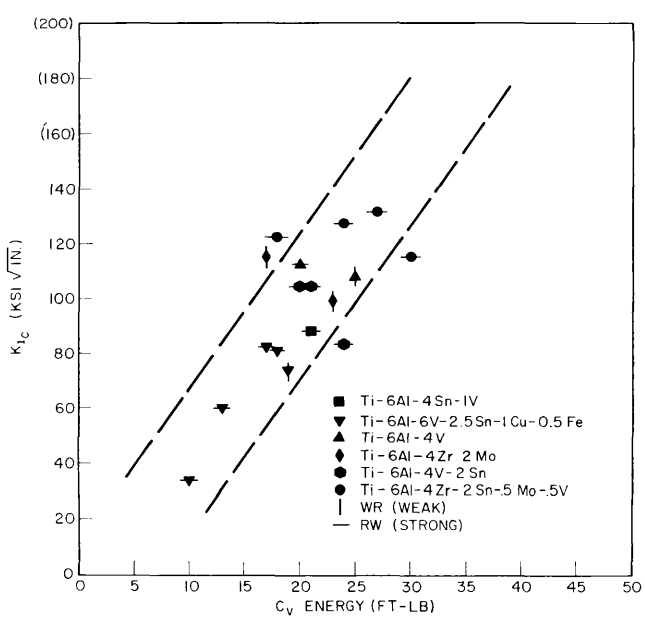

Fig. 9 - Correlation of K_{Ic} and C_v values (70°F) for 1-in.-thick plate

procuring the best quality material for the strength level of interest. The band between the two OMTL curves defined a corridor of fracture toughness-yield strength relationships. The corridor was recognized as an index of the strength transition of the family of alloys which provided for increased strength. The OMTL diagram was additionally indexed to include zones encompassing the DT data for different steels of primary interest. This zonal indexing served to define the strength-toughness characteristics for specific steels in relation to the OMTL corridor.

Critical flaw depths were calculated based on the K_{Ic} or K_c conditions relating to 1- and 3-in.-thick plate. These calculations provided an overlay of the OMTL diagram with iso-flaw depth lines for different conditions of flaw shape and stress level. In this manner then the DT, C_v, and K_{Ic} values could be interpretated directly to critical flaw size requirements for fracture. In the low fracture toughness region of the combined diagram, the flaw sizes clearly related to plane strain K_{Ic} conditions and were small. For the high fracture toughness region, the calculated flaw sizes were huge and related to full plane stress K_c conditions for fracture for the section sizes involved. Intermediate levels of fracture toughness corresponded to mixed-mode fracture; flaw sizes were relatively large, particularly for nominal stresses of less than yield-level magnitude.

It was mentioned earlier that the crack-tip plastic zone size is proportional to the ratio $(K_{Ic}/\sigma_{ys})^2$. Thus, the flaw size diagrams actually represent a system of iso-flaw depth lines which relate to the $(K_{Ic}/\sigma_{ys})^2$ ratio. The simple form of the ratio K_{Ic}/σ_{ys} thus provides for engineering assessment of flaw size-stress conditions for failure in a relatively simple fashion. This was demonstrated by indexing K_{Ic}/σ_{ys} ratio lines of 0.5, 1.0, 1.5, and 2 to the iso-flaw depth line diagrams. As a final step, interpretive diagrams of simple form were evolved which related failure conditions solely to the locus of the ratio lines. This procedure reduces an otherwise confusing combination of interacting parameters to a simple presentation. An example is given by the Ratio Analysis Diagram (RAD) developed for the generic classes of steels, Fig. 10. The following aspects of the RAD should be noted:

1. The fracture toughness scales are indexed to C_v, DT, and K_{Ic} parameters.

2. The OMTL corridor representing the strength transition is clearly evident.

3. The zonal location in the diagram of specific types of steels (HY-130, 9-4-0.20, 18% Ni marage, etc.) are clearly evident.

4. The ratio lines define the relative fracture toughness characteristics according to flaw size-stress required for fracture in terms of order of magnitude (see below), which are easily remembered and provide for "instant" assessment suitable for most engineering needs.

5. New data points can be indexed to the total diagram by entry from a desired scale. The relative quality of the metal is immediately made apparent.

As the K_{Ic}/σ_{ys} ratio increases, there is a dramatic increase in critical flaw size for failure. For example, ratio values below 0.5 correspond to critical flaw depths and widths in the order of hundredths of inches, even for nominally low elastic stress levels. Ratios between 0.5 and 1.0 relate to critical flaw depths of tenths of inches and widths ranging to several inches for load conditions involving high elastic stresses. For ratios of 1.0 to 1.5, critical flaw depths are in the order of inches, and plastic deformation is required for fracture propagation in a plane stress mode for a 1-in. thick plate. Above ratios of 2.0, the critical flaw sizes become huge in relation to section thickness of 1- to 3-in. plates. All that is necessary is to realize this fact and that there is no need for calculation — in any event, a large plastic overload is required for fracture propagation.

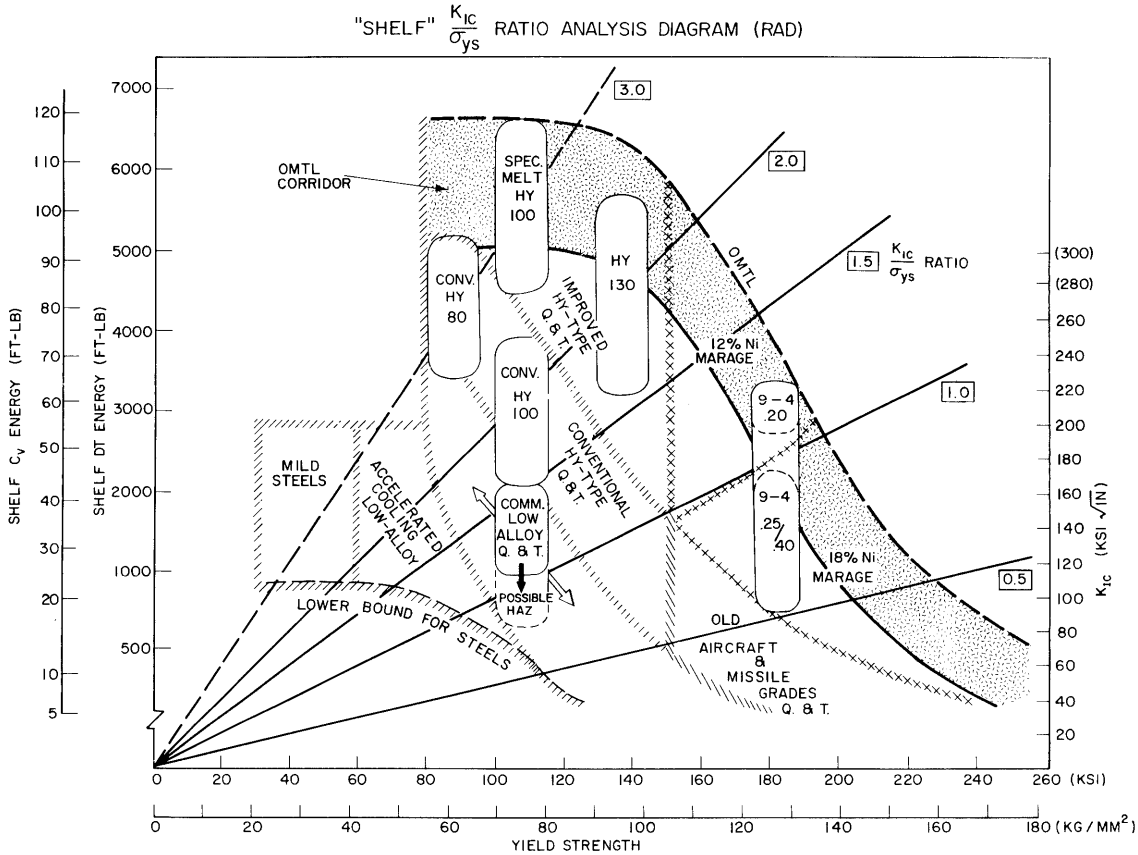

Fig. 10 - Compendium RAD indexed for the generic classes of steels (Ref. 1)

Similar analyses have been made for titanium alloys and are presented in the following sections.

Fracture Toughness Diagram for Titanium Alloys

Compared to steels, titanium alloys do not show a sharp transition in fracture toughness with increasing temperature — only a gradual change is noted over a relatively broad range of temperature. This gradual change in fracture toughness is illustrated in Fig. 11, in which a large body of C_v data is summarized with respect to broad ranges of yield strength.

The fracture toughness OMTL diagram for 1-in.-thick plate, which includes data for all the different generic families of titanium alloys, is shown in Fig. 12. The data represent as-rolled material and a variety of processing and heat-treatment conditions for alloys in each family.

The upper OMTL curve relates to the highest "weak" direction fracture toughness values determined for the related level of yield strength. The normal expectancy OMTL curve relates to the level of fracture toughness that can be expected with reasonable confidence if the best of chemistry, processing, and heat treatment are specified. The range of fracture toughness indicated for any given level of yield strength results from chemical composition, impurities, processing, and heat-treatment variables. The

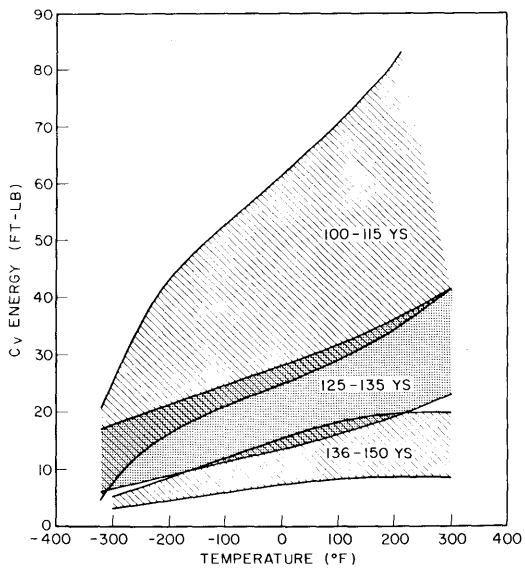

Fig. 11 - Summary relationships of C_v curves for broad ranges of yield strength in titanium alloys

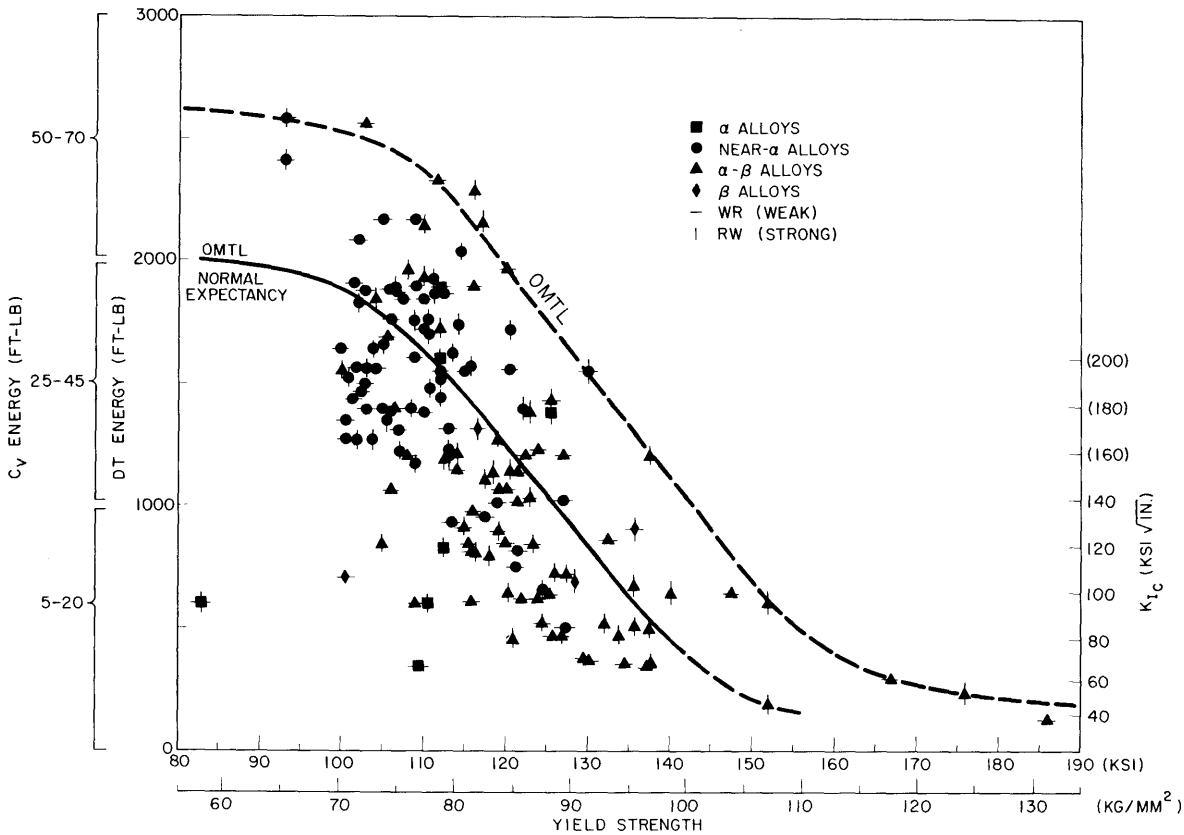

Fig. 12 - OMTL diagram for titanium alloys. Data points relate to 1-in. thick DT test values. The other fracture toughness scales are indexed to DT energy by correlation.

relative effects of these variables become evident by noting the relative position of the specific material in the diagram. Melt practice is not considered a major factor as for steels, since double-vacuum-arc melting is the only commercial process for titanium.

The OMTL diagram data points represent DT test measurements. The use of the DT test for the bulk of the characterization process was required because of the difficulties of using C_v data and the high cost of K_{Ic} tests. Additionally, the DT tests provide for presenting the total spectrum of toughness which direct use of K_{Ic} tests cannot provide. The K_{Ic} scale on the right side of the diagram is obtained from the K_{Ic}-vs-DT correlation plot. The high K_{Ic} values in parentheses represent the extrapolated portion of the K_{Ic}-vs-DT plot. The C_v range scale on the left side of the diagram was obtained from the DT-vs-C_v correlation diagram. The scales were positioned according to the correlations. Entrance into the diagram can be made from any of these scales for which data are available. Obviously, the yield strength of the material must be known to index the data point in the diagram.

The general behavior of titanium alloys in the ETT presented in Fig. 4 for high, intermediate, and low fracture toughness corresponds to OMTL corridor material at about 100-, 130-, and 150-ksi yield strength. The dramatic change in fracture toughness represented by the OMTL corridor strength transition of titanium alloys becomes clearly evident from this illustration.

Flaw Size Analysis Diagram

A typical Flaw Size Analysis Diagram for titanium alloy plate is presented in Fig. 13 for a 1:10 (depth-to-length) semi-infinite flaw and for yield stress loading. Figure 14 presents relationships for one-half yield stress loading. The OMTL corridor of the previous chart is used for purposes of reference. The diagrams feature critical iso-flaw depth lines calculated for both 1- and 3-in.-thick plate considering K_{Ic} or K_c conditions as appropriate. The lines are positioned on the diagram from calculations derived from the K_{Ic} scale. Approximate critical flaw depths relating to the 1:2 "thumbnail" geometry flaw can be deduced by multiplication of the indicated 1:10 flaw depth by a factor of 2.5.

The critical flaw depth-stress calculations are considered to be reasonably accurate for K_{Ic} values up to 140 ksi $\sqrt{\text{in.}}$ for 1- to 3-in.-thick plate. The calculations for K_{Ic} values above 140 ksi $\sqrt{\text{in.}}$ have been adjusted to account for the increased effects of mixed-mode and full plane stress K_c conditions involved. The formal relationships for K_{Ic}-to-K_c calculations are recognized to represent approximations; thus, accuracy is not claimed for the critical flaw depth sizes indicated in this region. In addition, the K_{Ic} values in this range also involve approximations for reasons explained earlier. Therefore, the flaw size-stress relationships indicated for K_{Ic} values above 140 ksi $\sqrt{\text{in.}}$ serve only to define conditions which do not require exact calculation. The critical flaw sizes calculated for this region should provide adequate information for most engineering purposes.

By following the OMTL corridor from low to high strength, a sharp drop in critical flaw size may be noted in the region of 120- to 140-ksi yield strength. Very high plane stress fracture toughness and corresponding huge flaw sizes associated with plastic overload characterize OMTL corridor material below 120-ksi yield strength. Above 140-ksi yield strength brittle fracture may occur from minute flaws in the order of tenths or hundredths of inches. From these comparisons it is obvious that in the range of 120- to 140-ksi yield strength there is a major premium to be gained using the very best materials available.

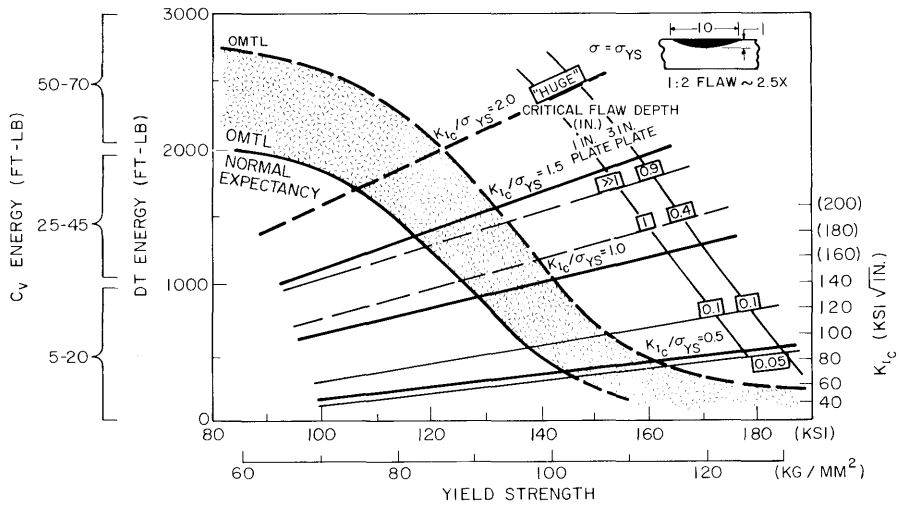

Fig. 13 - Calculated iso-flaw depth lines for 1:10 surface cracks and yield stress loading superimposed on the OMTL corridor diagram. Calculations apply specifically to 1- and 3-in.-thick material. For 1:2 flaw geometry multiply the indicated crack depth values by 2.5.

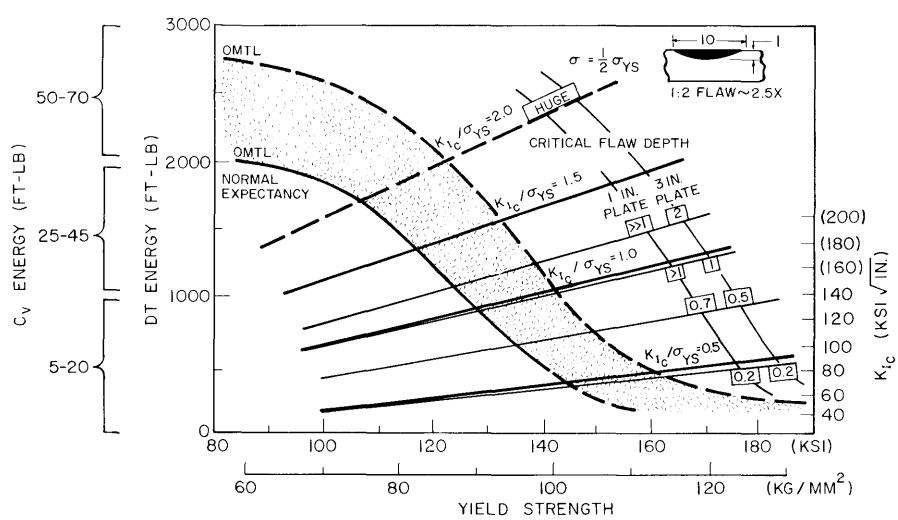

Fig. 14 - Calculated iso-flaw depth lines for 1:10 surface cracks and one-half yield stress loading. The comments of Fig. 13 apply.

The flaw size diagrams are zoned by K_{Ic}/σ_{ys} ratio lines of 0.5, 1.0, 1.5, and 2.0. These ratio lines define five zones of rapidly changing fracture toughness and critical flaw size. As discussed previously, the K_{Ic}/σ_{ys} ratio lines follow the slope of the iso-flaw depth lines, since the K_{Ic}-to-σ_{ys} ratio is the basic parameter in the equations used for calculating flaw size and for defining fracture toughness.

By substituting the ratio lines for the iso-flaw depth lines, a simplified engineering analysis of fracture toughness can be made as follows:

1. Above the ratio line of 2, nominal stresses in excess of yield and crack lengths many times the plate thickness are required for fracture. This requirement follows because full plane stress conditions are expected to exist even for 3-in. thickness.

2. For ratios between 1.5 and 2, nominal stresses above yield and through-thickness flaws with lengths well in excess of the plate thickness are required for 1-in.-thick material for reasons cited above. Flaws in the order of an inch to several inches in depth and lengths in excess of plate thickness are required for fracture of 3-in.-thick plate. Mixed-mode plane stress conditions will prevail for the 3-in. plate thicknesses.

3. In the range of 1.0 to 1.5 ratios, stresses in excess of yield and through-thickness flaws with lengths in excess of the plate thickness are required for fracture propagation in the mixed plane stress mode for 1-in. plate.

4. For ratios of 0.5 to 1, critical flaw depths in the order of tenths of inches are sufficient to cause plane strain fracture at relatively high levels of elastic stress for both 1- and 3-in. thickness.

5. Below the 0.5 ratio line, relatively low elastic stresses and minute flaws (critical flaw depth in the order of hundredths of inches) are sufficient to initiate and propagate plane strain fractures for both 1-in. and 3-in. thickness.

A further simplification can be made which is applicable for 1- to 3-in. sections for most engineering purposes:

1. $K_{Ic}/\sigma_{ys} > 1.5$ — no need to calculate; flaw sizes are very large and associated with plastic loading.

2. $K_{Ic}/\sigma_{ys} < 1.5$ but >0.5 — use Flaw Size Analysis Diagrams for best definition of approximate critical flaw size and stress.

3. $K_{Ic}/\sigma_{ys} < 0.5$ — critical flaw sizes are very small and may be below reliable detectability limit.

Ratio Analysis Diagram

The K_{Ic}/σ_{ys} RAD for titanium alloys was evolved from the definition of the engineering significance of the ratio as described in the previous section. The RAD is presented in Figs. 15 and 16 to describe the general fracture toughness characteristics of several principal near-α and α-β alloys, respectively. All available DT data for 1-in.-thick plate of the indicated alloys are encompassed in zonal locations of the OMTL corridor diagram. The zones also include limited DT data for the alloys Ti-7Al-2Cb-1Ta, Ti-6Al-2Cb-1Ta-0.8Mo, and Ti-6Al-4V in 2-1/2- to 3-in.-thick plate. Analysis of sections greater than 1 in. presumes that a 1-in. DT test was made for the material. For any particular alloy, variations of strength and toughness within a zone reflect differences in chemistry, processing, and heat treatment.

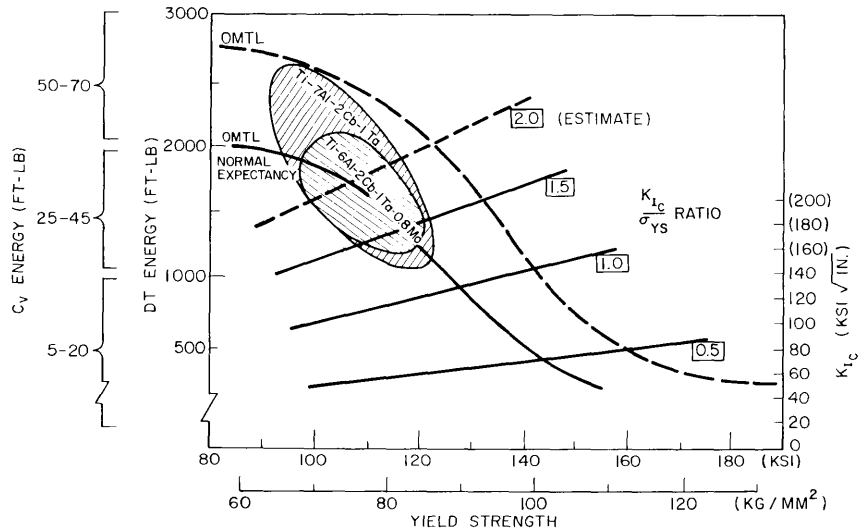

Fig. 15 - RAD superimposed on OMTL corridor diagram showing zonal locations of DT data for several principal near-α titanium alloys

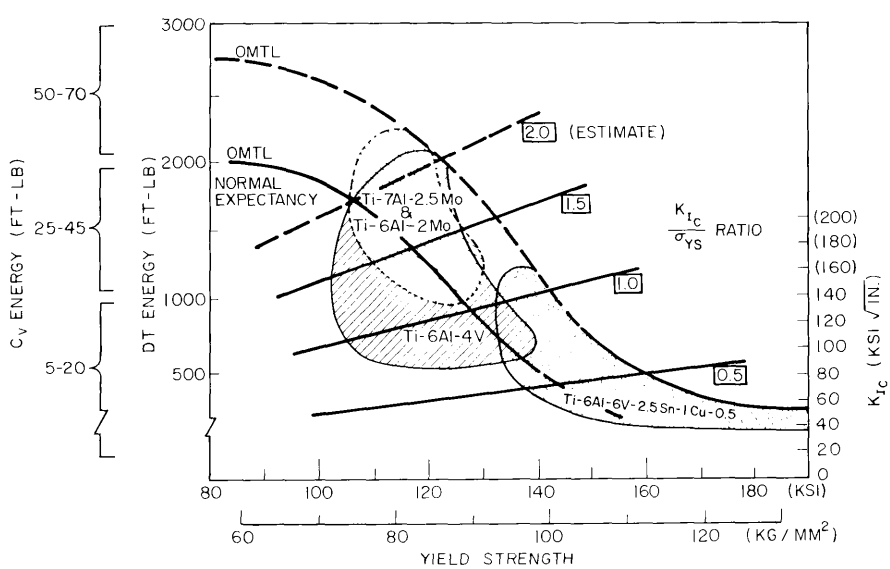

Fig. 16 - RAD superimposed on OMTL corridor diagram showing zonal location of DT data for several principal α-β titanium alloys

All titanium alloys of interest for structural applications have yield strengths in the range of 80 to about 180 ksi. To cover this strength range with the required ratio lines, a linear scale of K_{Ic} is used for values below 40 ksi $\sqrt{in}$. This represents an expansion of the scale used in the Flaw Size Analysis Diagrams.

The zonal locations of the Ti-7Al-2Cb-1Ta and Ti-6Al-2Cb-1Ta-0.8Mo alloys in Fig. 15, with respect to the ratio lines indicate very high fracture toughness capabilities for these alloys below 110-ksi yield strength. Large to huge flaws and general plastic yielding are required for fracture. Due to the metallurgical nature of these alloys, yield strengths above 130 ksi would be difficult to obtain in thick sections and then only with an unacceptable sacrifice in fracture toughness.

The α-β alloys are generally designed for use at yield strength levels above 140 ksi. The zones for the Ti-7Al-2.5Mo, Ti-6Al-2Mo, and Ti-6Al-4V alloys shown in Fig. 16 reflect recent attempts to optimize these alloys for use in the range of 110- to 130-ksi yield strength. An increase in strength in this range is shown to be accomplished by a gradual decrease in the general level of fracture toughness.

The upper boundary of the zonal regions for the α-β alloys indicated above is shown to lie in the OMTL corridor from 100- to 140-ksi yield strength. Obtaining this high level of toughness requires interstitial oxygen concentrations below 0.08 wt-% maximum. At the average oxygen level of 0.12% for ELI grade material, K_{Ic}/σ_{ys} ratios of 1.5 would be difficult to obtain, and ratios of about 1.0 would normally be expected at 120-ksi yield strength.

The relatively new ultrahigh-strength α-β alloy Ti-6Al-6V-2.5Sn-1Cu-0.5Fe follows the present OMTL corridor in the ultrahigh-strength region of the diagram.

A compendium RAD which summarizes all fracture toughness information for the generic families of titanium alloys is shown in Fig. 17 for 1-in.-thick plate. The zonal locations indicated for each family are based on all available DT data and cover the yield strength and fracture toughness range generally encountered with current alloys and processing techniques. The limited DT data mentioned earlier for thicker sections of several near-α and α-β alloys indicate that the same general zonal regions can be expected to apply for thicknesses up to 3 in.

OMTL corridor quality material is obtained with α and near-α alloys up to about 110-ksi yield strength. Above 110-ksi yield strength, the fracture toughness of both types of α alloys begins to fall rapidly away from the OMTL corridor, and optimum properties are no longer obtainable. This rapid drop in fracture toughness for these alloys is illustrated by the upper zone region dropping from a K_{Ic}/σ_{ys} ratio of well over 2 at 100-ksi yield strength to almost 0.5 at 130-ksi yield strength.

Alloys of the α-β type define the OMTL corridor from 110- to about 190-ksi yield strength. As stated earlier, in the 110- to 140-ksi yield strength range, OMTL corridor levels of fracture toughness in these alloys are seen as requiring very low levels of interstitial oxygen content and optimum processing.

The β alloys are also expected to follow the OMTL corridor in the ultrahigh yield strength range. Limited data for several β alloys currently under development indicate that in the lower yield strength range of 110 to 130 ksi, the level of fracture toughness will be below that of the best α-β alloys but that K_{Ic}/σ_{ys} ratios in the order of 1.0 to 1.5 should be obtainable.

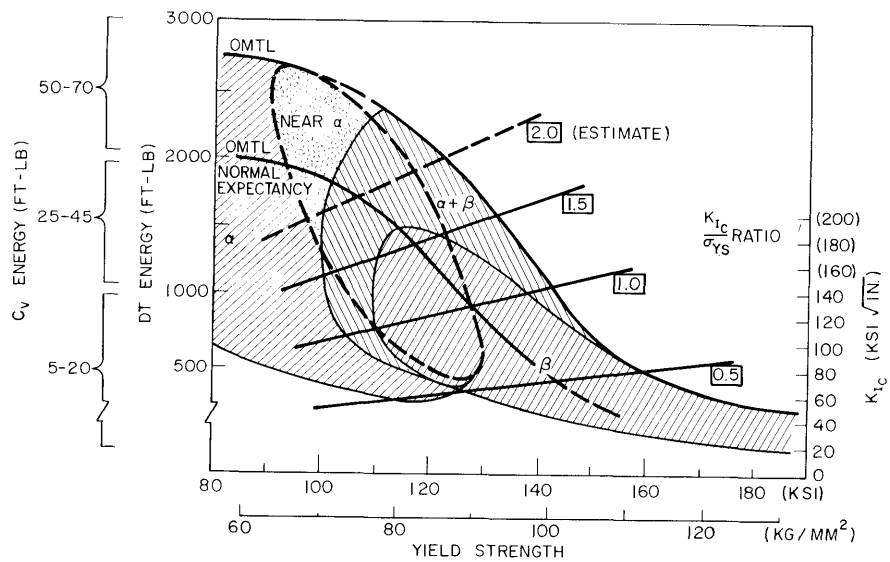

Fig. 17 - Compendium RAD for generic classes of titanium alloys

SUMMARY

Fracture mechanics analytical procedures provide for characterizing the fracture toughness of high-strength titanium alloys in terms of critical flaw size-stress level for fracture. Unfortunately, strictly valid characterizations are restricted to relatively brittle alloys at the present state of development of fracture mechanics. These restrictions derive from the transition from plane strain to plane stress fracture as toughness is increased with retention of section size in the range of 1- to 3-in. thickness. As a separate but practical consideration, fracture mechanics tests are essentially research tools and are too expensive for routine engineering usage.

Analysis of flaw size-stress relationships indicates that for most engineering purposes the exact definition of conditions for fracture required for failure-safe design with brittle materials is not necessary for materials which feature relatively high fracture toughness. This suggests the use of a two-step approach based on correlations between simple engineering tests and fracture mechanics tests. The first step is the development of procedures by which interpretation of the tests could be made in terms of critical flaw size for fracture. The second step is the evolution of simplified and easily remembered interpretative procedures for flaw size-stress level requirements for fracture based on the K_{Ic}/σ_{ys} ratio. Thus, the two-step correlation procedure provides a practical way for extending the estimate of plane strain K_{Ic} conditions to mixed-mode and full plane stress K_c conditions for fracture in a manner which is satisfactory for most engineering purposes.

Interpretative procedures are evolved from the correlation of K_{Ic} with the DT and C_v fracture toughness tests for 1-in.-thick plate. In the region of low fracture toughness corresponding to a condition of high mechanical constraint (plane strain), the correlations are reasonably accurate. Beyond the region of strictly valid K_{Ic} measurements, the correlations are extrapolated to provide for interpretation of C_v and DT values to expected K_{Ic} values for limited increase in plate thickness.

A master OMTL diagram has been developed which summarizes all fracture toughness information on 1-in.-thick plate in terms of DT energy. The DT energy is indexed by C_v and K_{Ic} according to the correlation plots. An OMTL limit curve indicating the highest level of fracture toughness attained for any level of yield strength is defined by the DT data. A normal expectancy OMTL curve is also indicated which denotes the level of fracture toughness that can be reasonably expected when procuring the best quality material.

Flaw Size Analysis Diagrams are developed which feature critical flaw size calculations for 1- and 3-in.-thick plate according to conditions of K_{Ic} or K_c as appropriate. The calculations are used to index the DT, C_v, and K_{Ic} scales of the OMTL diagram by superimposing iso-flaw depth lines on the diagram. For the low fracture toughness range, the critical flaw sizes are indicated as fractions of inches; for the high fracture toughness region, these are indicated to be very large and do not require calculation.

All of the preceding aspects are simplified further for a general engineering interpretation of flaw size-stress level for fracture by evolving the K_{Ic}/σ_{ys} RAD and coupling it to the OMTL diagram. The ratio is indexed to the flaw size calculations; thus, the coupling provides for establishing the significance of the zonal locations of high-strength titanium alloys of special interest with respect to flaw size-stress level for fracture. Based on all available data as well as the general physical metallurgy aspects of high-strength titanium alloys, a compendium RAD is evolved for the generic classes of titanium alloys which defines the yield strength range for optimum properties of each class of alloy.

ACKNOWLEDGMENTS

The authors are indebted to Mr. W. S. Pellini for his interest and helpful discussions concerning various aspects of these investigations. Mr. C. R. Forsht and Mr. A. J. Kuntz were responsible for specimen preparation, heat treatment, and performing many of the tests. The authors are also grateful to the Office of Naval Research, Naval Ship Systems Command, Code 0342, and Deep Submergence Systems Project, Code 221, for their interest and financial support for this work.

REFERENCES

1. Pellini, W.S., "Advances in Fracture Toughness Characterization Procedures and in Quantitative Interpretations to Fracture-Safe Design for Structural Steels," Welding Research Council Bulletin, Series 130, May 1968

2. Paris, P.C., and Sih, G.C., "Stress Analysis of Cracks," ASTM Special Technical Publication 381, Fracture Toughness Testing and Its Applications, American Society for Testing and Materials, Philadelphia, Pennsylvania, pp. 30-81, 1965

3. Brown, W.F,, Jr., and Srawley, J.E., "Plane Strain Crack Toughness Testing of High Strength Metallic Materials," ASTM Special Technical Publication 410, American Society for Testing and Materials, Philadelphia, Pennsylvania, 1966

4. Pellini, W.S., et al., "Review of Concepts and Status of Procedures for Fracture-Safe Design of Complex Welded Structures Involving Metals of Low to Ultrahigh Strength Levels," NRL Report 6300, June 1965

Appendix

CHARACTERISTICS OF COMMERCIALLY PRODUCED TITANIUM ALLOYS REFERENCED IN REPORT

Alloy Type	NRL Alloy Reference No.	Nominal Yield Strength Range Investigated (ksi)	Chemical Composition (wt-%)															
			Al	Sn	V	Mn	Fe	Mo	Cb	Ta	Zr	Mg	Cu	Si	O_2	N_2	C	H_2
α-Alloys																		
5Al-2.5Sn		110-125																
	T-3		5.49	2.46	–	0.01	0.20	–	–	–	–	0.007	–	0.034	0.07	0.12	0.033	0.018
	T-18		5.18	2.56	–	–	0.08	–	–	–	–	–	–	–	0.07	0.013	0.032	0.008
Near-α Alloys																		
6Al-2Cb-1Ta-0.8Mo		95-120																
	T-96		6.0	–	–	0.01	0.07	0.75	2.3	1.1	–	–	–	–	0.055	0.005	0.02	0.004
	R-6		6.0	–	–	–	0.07	0.77	2.0	1.1	–	–	–	–	0.081	0.009	0.02	0.005
7Al-2Cb-1Ta		100-120																
	T-33		7.2	–	–	0.33	–	0.11	2.4	1.0	–	–	–	0.13	0.071	0.01	0.02	–
	T-73		6.9	–	–	–	0.13	–	2.5	1.1	–	–	–	–	0.063	0.006	0.01	–
	T-82		6.9	–	–	–	0.13	–	2.4	1.1	–	–	–	–	0.068	0.01	0.02	–
	T-89		6.6	–	–	–	0.1	–	2.6	1.3	–	–	–	–	0.07	0.008	0.026	0.003
8Al-2Cb-1Ta		100-120																
	T-11		8.3	–	–	–	0.13	–	1.9	0.86	–	–	–	–	0.06	0.01	0.02	–
	T-23		8.0	–	–	–	0.13	–	2.0	1.0	–	–	–	–	0.06	0.01	0.02	0.007
	T-44		8.32	–	–	–	0.17	–	2.47	2.07	–	–	–	–	0.086	0.006	0.02	–
6.5Al-5Zr-1V	T-36	100-115	6.3	–	1.0	–	0.06	–	–	–	4.8	–	–	–	0.06	0.006	0.023	0.008
6Al-4Zr-2Sn-0.5Mo-0.5V	T-68	110-115	6.0	1.9	0.5	–	0.05	0.48	–	–	4.4	–	–	–	0.073	0.01	0.02	0.003
6Al-4Sn-1V	T-20	100-115	6.0	3.9	1.0	–	0.05	–	–	–	–	–	–	–	0.062	0.010	0.024	0.003
6Al-4Zr-1V	T-24	100-115	5.79	–	1.0	–	0.08	–	–	–	3.76	–	–	–	0.064	0.015	0.022	0.004
α-β Alloys																		
6Al-4V		105-140																
	T-5		5.85	–	3.85	0.03	0.19	–	–	–	–	Trace	–	0.033	0.06	0.06	0.042	0.005
	T-91		6.0	–	4.0	–	0.05	–	–	–	–	–	–	–	0.08 Max.	0.09	0.023	–
	T-95		5.9	–	4.0	–	0.10	–	–	–	–	–	–	–	0.114	0.013	0.022	0.005
	T-100		5.7	–	4.0	–	0.07	–	–	–	–	–	–	–	0.07	0.01	0.022	0.007
6Al-2Mo		105-130																
	T-22		5.6	–	–	–	0.06	2.2	–	–	–	–	–	–	0.062	0.015	0.028	0.004
	T-59		5.9	–	–	–	0.06	1.6	–	–	–	–	–	–	0.06	0.012	0.03	0.003
	T-99		6.1	–	–	–	0.04	1.9	–	–	–	–	–	–	0.07	0.012	0.029	0.003
	R-1		6.0	–	–	–	0.02	1.9	–	–	–	–	–	–	0.09	0.008	0.025	0.008
7Al-2.5Mo		105-130																
	T-71		6.8	–	–	–	0.04	2.4	–	–	–	–	–	–	0.06	0.008	0.023	0.004
	T-94		6.9	–	–	–	0.04	2.6	–	–	–	–	–	–	0.073	0.008	0.023	0.0055
7Al-1Mo-1V		115-125																
	T-88		6.9	–	0.9	–	0.04	1.0	–	–	–	–	–	–	0.07	0.010	0.022	0.007
	R-8		6.8	–	1.2	–	0.03	1.0	–	–	–	–	–	–	0.08	0.007	0.021	0.006
8Al-1Mo-1V	T-19	115-125	7.96	0.15	1.0	–	0.12	0.90	–	–	–	–	–	–	0.07	0.013	0.049	0.006
6Al-4V-2Sn	T-67	115-120	6.1	2.0	3.9	–	0.07	–	–	–	–	–	–	–	0.08	0.01	0.03	0.005
6Al-3V-1Mo	T-93	105-120	5.9	–	3.1	–	0.05	1.0	–	–	–	–	–	–	0.07	0.007	0.022	0.006
6Al-4V-2Mo	R-2	125-130	5.9	–	4.1	–	0.03	2.1	–	–	–	–	–	–	0.06	0.008	0.023	0.005
6Al-2Sn-1Mo-1V		100-125																
	T-25		5.69	1.92	0.96	–	0.08	1.10	–	–	–	–	–	–	0.065	0.010	0.025	0.005
	T-37		5.8	2.0	1.0	–	0.064	1.1	–	–	–	–	–	–	0.07	0.008	0.023	0.007
6Al-4Zr-2Mo	T-55	115-125	6.0	–	–	–	0.07	1.9	–	–	3.8	–	< 0.2	–	0.083	0.01	0.01	0.008
4Al-3Mo-1V	R-3	110-130	4.0	–	1.2	–	0.03	3.1	–	–	–	–	–	–	0.08	0.009	0.023	0.005
6Al-6V-2Sn-1Cu-0.5Fe		135-190																
	T-21		5.5	2.0	5.5	–	0.69	–	–	–	–	–	0.73	–	0.08	0.010	0.024	0.003
	T-92		5.6	2.0	5.3	–	0.52	–	–	–	–	–	0.92	–	0.067	0.01	0.022	0.007
6Al-6V-2Sn-2Mo	R-4	135-145	6.0	2.0	6.1	–	0.06	2.1	–	–	–	–	–	–	0.08	0.011	0.023	0.007
5Al-2Sn-2Mo-2V	T-90	110-120	4.9	2.2	1.9	–	0.06	1.9	–	–	–	–	–	–	0.057	0.009	0.023	0.012
β Alloys																		
11Mo-5Sn	R-10	90-155	–	5.0	–	–	0.09	11.3	–	–	–	–	–	–	0.05	0.009	0.025	0.003
11Mo-5.5Sn-5Zr	R-11	108-115	–	4.8	–	–	0.06	11.0	–	–	4.9	–	–	–	0.07	0.004	0.018	0.003

Security Classification

DOCUMENT CONTROL DATA - R & D

(Security classification of title, body of abstract and indexing annotation must be entered when the overall report is classified)

1. ORIGINATING ACTIVITY *(Corporate author)* Naval Research Laboratory Washington, D.C. 20390	2a. REPORT SECURITY CLASSIFICATION Unclassified 2b. GROUP

3. REPORT TITLE

PROCEDURES FOR FRACTURE TOUGHNESS CHARACTERIZATION AND INTERPRETATIONS TO FAILURE-SAFE DESIGN FOR STRUCTURAL TITANIUM ALLOYS

4. DESCRIPTIVE NOTES *(Type of report and inclusive dates)*
Interim report; work is continuing

5. AUTHOR(S) *(First name, middle initial, last name)*

R.J. Goode, R.W. Judy, Jr., and R.W. Huber

6. REPORT DATE December 5, 1968	7a. TOTAL NO. OF PAGES 28	7b. NO. OF REFS 4
8a. CONTRACT OR GRANT NO. NRL Problem M01-05 and F01-17 b. PROJECT NO. SF 51-541-004-12386 c. SF 51-541-005-12393 DSSP S-4607-11894 d. RR 007-01-46-5405	9a. ORIGINATOR'S REPORT NUMBER(S) NRL Report 6779 9b. OTHER REPORT NO(S) *(Any other numbers that may be assigned this report)*	

10. DISTRIBUTION STATEMENT

This document has been approved for public release and sale; its distribution is unlimited.

11. SUPPLEMENTARY NOTES	12. SPONSORING MILITARY ACTIVITY Department of the Navy (Naval Ship Systems Command, Office of Naval Research, and Deep Submergence Systems Project), Washington, D.C. 20360

13. ABSTRACT

Interpretations of fracture toughness characteristics, as measured by various test procedures, for solutions of general engineering problems are presented for structural titanium alloys. Analytical procedures evolved from fracture mechanics theory are used for quantitative interpretations of engineering fracture toughness tests. The procedural simplicity of the engineering tests coupled with the analytical capabilities of fracture mechanics theory provides for a significant advancement in failure-safe design procedures for titanium alloys covering the full range of strength levels.

Interpretative procedures are evolved from correlations of K_{Ic} with Dynamic Tear (DT) and Charpy-V notch (C_v) energy. An Optimum Materials Trend Line (OMTL) diagram is developed for titanium alloys which summarizes all the DT fracture toughness data and is additionally indexed according to the K_{Ic} and C_v correlation plots. The OMTL limit curves are shown for the best and normally expected grades of material for the strength level.

Flaw size-stress calculations for fracture of 1- and 3-in.-thick sections are overlayed to the OMTL diagram in the form of iso-flaw depth lines. K_{Ic}/σ_{ys} ratio lines are indexed to the iso-flaw depth lines, and a K_{Ic}/σ_{ys} Ratio Analysis Diagram

(over)

DD FORM 1 NOV 65 1473 (PAGE 1)

S/N 0101-807-6801

Security Classification

Security Classification

14. KEY WORDS	LINK A ROLE	LINK A WT	LINK B ROLE	LINK B WT	LINK C ROLE	LINK C WT
Fracture mechanics						
Dynamic tear test						
Charpy-V notch test						
Titanium alloys						
Fracture toughness tests						
Optimum Materials Trend Line diagram						
Ratio Analysis Diagram						

(RAD) is evolved. The RAD provides for a simplified, general engineering interpretation of flaw size-stress conditions for fracture.

The general fracture toughness characteristics of some principal titanium alloys are simply defined by zones in the RAD. A compendium of such zones provides a general understanding of the potentials for each generic class of titanium alloys.

DD FORM 1 NOV 65 1473 (BACK)
(PAGE 2)

Security Classification